Progress In Electromagnetics Research Letters, Vol. 109, 57–63, 2023

A Novel Highly Selective UWB Bandpass Filter Using Quad-Mode Stub-Loaded Resonator

Guang Yong Wei[1], Yun Xiu Wang[1,*], Jie Liu[1,2], Yang Gao[1], and Xiao Tao Yao[1]

Abstract—In this letter, a novel ultra-wideband (UWB) bandpass filter (BPF) configuration with a quad-mode resonator (QMR) structure is proposed, which has a highly selective and compact performance. The QMR is composed of a funnel-shaped resonator loaded in the middle and a low-impedance folded microstrip line. Initially, the resonant frequencies are uniformly distributed in the UWB passband by varying the length of QMR physical stubs, and later three-line parallel coupled lines are employed to enhance coupling to obtain a flat passband. The feed lines are then loaded with a pair of $\lambda/2$ stepped impedance radial stubs (SIRSs) to provide excellent band-stop characteristics. Finally, a filter prototype is created, and its performance is evaluated using the generated data. The proposed UWB filter has sharp roll-off ratio of 99 and 63 dB/GHz, respectively, at the lower and upper edges of the passband.

1. INTRODUCTION

The unlicensed 3.1 to 10.6 GHz operational frequency band was authorized by the Federal Communications Commission (FCC) in 2002 [1], which encouraged researchers to develop a variety of ultra-wideband (UWB) technology applications, including communications and positioning systems, as well as medical imaging devices UWB bandpass filters are crucial components of communication systems. Its advancement has raised many concerns since it can efficiently eliminate out-of-band interference signals and ensure the integrity of UWB transmission. For the development of UWB filters, the comprehensive design approach of conventional narrowband filters is no longer appropriate. Today, numerous researchers use several methods to create UWB filters, and multi-mode resonator (MMR) technology is one of the most extensively used and promising approaches [2–10]. By combining microstrip lines of various impedances to create an MMR unit in [2], the authors demonstrate how the first three resonant frequencies can be used to create a UWB passband by altering the MMR impedance ratio and using strong coupling. In [3–5], four-mode resonators were used to develop UWB filters with broad upper stopbands; however, the proposed filters' selectivity was not particularly excellent. Later in [6], selectivity-improved UWB filters are designed using a two-stage harpoon-shaped resonator based on a multimode resonator. Ultra-wideband filters with both high selectivity and wide stopband were also later implemented in [7–10]. Compact hybrid microstrip/co-planar waveguide technology using a substrate bilayer was employed to reduce the circuit size [11–13]. However, this form of UWB filter is susceptible to harmonic effects, which lead to unfavorable stopbands.

We propose a novel UWB-BPF based on a quad-mode resonator (QMR) with sharp rejection skirt in this manuscript, using stepped impedance radial stubs to improve passband edges with poor selectivity. The suggested structure has a relative dielectric constant of 3.38, a height of 0.8 mm, and a loss tangent of 0.003 and was created and optimized using the Advanced Design System (ADS) for

Received 5 January 2023, Accepted 16 February 2023, Scheduled 28 February 2023

* Corresponding author: Yun Xiu Wang (627662147@qq.com).
[1] School of Electronic and Information Engineering, China West Normal University, Nanchong 637009, China. [2] School of Physics and Astronomy, China West Normal University, Nanchong 637009, China.

an F4BM-2 substrate, which is inexpensive and widely accessible. The proposed BPF is made, and the measurements supporting it are confirmed.

2. DESIGN OF PROPOSED UWB BPF

Figure 1 depicts the architecture of the proposed UWB BPF. As depicted in Figure 1, the quad-mode resonator (QMR) consists of a funnel-shaped open stub loaded at the center of a folded low-impedance microstrip line and a pair of SIRSs loaded on both sides of a three-line parallel coupled line. The frequency characteristics of the QMR with a funnel-shaped open stub are exploited to place the resonant modes within the UWB passband.

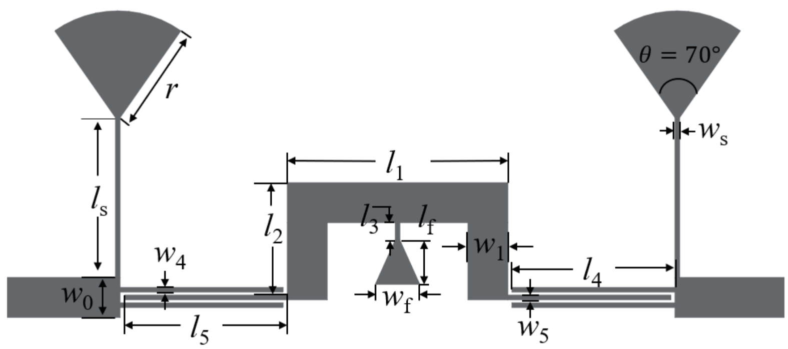

Figure 1. The architecture of the proposed UWB BPF.

The equivalent transmission line model of the proposed UWB BPF is depicted in Figure 2, in which the three parallel coupled lines can be equaled as a J-inverter susceptance in the middle and two parallel transmission lines at the two sides [14].

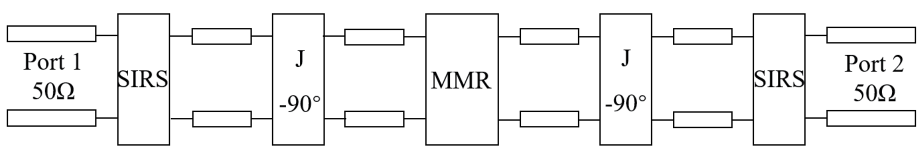

Figure 2. Equivalent transmission line model of the filter.

Considering that the resonator is symmetrical about A-A' plane, the odd and even mode method can be applied to analyzing it. For simplicity, we equate the electrical length of the funnel-shaped open stub to θ_f, as depicted in Figure 3.

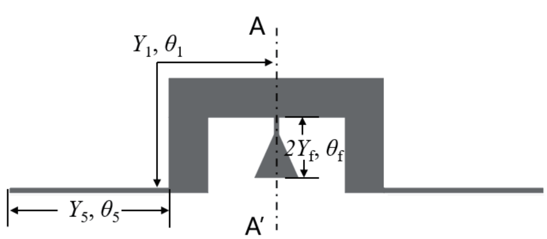

Figure 3. Basic quad-mode resonator (QMR).

When odd-mode excitation is applied, the central symmetry plane A-A' of the resonator is short-circuited, and Figure 4(a) depicts the odd-mode equivalent circuit.

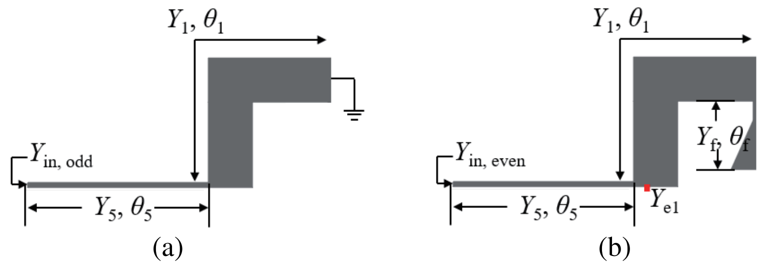

Figure 4. (a) Odd mode equivalent circuit of the QMR. (b) Even mode equivalent circuit of the QMR.

The input admittance for the odd mode can be expressed as

$$Y\text{in, odd} = -\text{j}\text{Y}_5 \frac{\text{Y}_1 \cot\theta_1 - \text{Y}_5 \tan\theta_5}{\text{Y}_5 + \text{Y}_1 \cot\theta_1 \tan\theta_5} \tag{1}$$

As a result, it can be determined that the odd modes are fixed and independent of the funnel-shaped open stub resonator form. The symmetrical plane A-A' should be open-circuited under the even mode of excitation, and Figure 4(b) depicts the even mode equivalent circuit.

The input admittance for the even mode can be calculated using

$$Y_{\text{in, even}} = Y_5 \frac{Y_{\text{el}} + jY_5 \tan\theta_5}{Y_5 + jY_{\text{el}} \tan\theta_5} \tag{2}$$

where

$$Y_{\text{e1}} = Y_1 \frac{jY_{\text{f}} \tan\theta_{\text{f}} + jY_1 \tan\theta_1}{Y_1 - Y_{\text{f}} \tan\theta_{\text{f}} \tan\theta_1} \tag{3}$$

The funnel-shaped open stub at the center position is related to the even-mode frequencies. The resonant frequencies of the odd and even modes can be calculated using the resonant conditions by setting (1) and (2) equal to 0. Figure 5 depicts the S_{21} amplitude of the resonator for weak coupling with $l_4 = 1$ mm, $w_4 = 0.2$ mm, and a minimum coupling gap of 0.15 mm to investigate its frequency response behavior.

We can observe from Figure 5(a) that there are four resonant frequencies in the UWB. It can be seen that the four resonant modes can be shifted by varying the dimension of l_2. The effect of l_f on

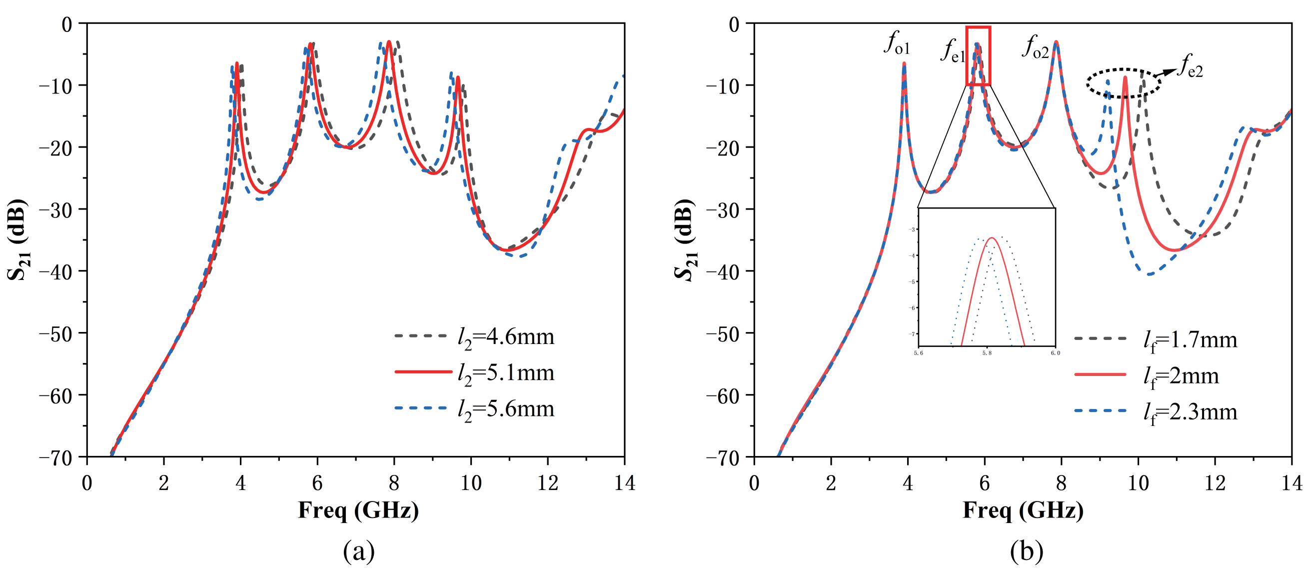

Figure 5. Frequency response under weak coupling. (a) L_2 length variation, (b) L_f length variation.

resonating modes is illustrated in Figure 5(b). l_f is an important parameter to contribute to the higher cut-off frequency of the proposed resonator. It has an influence on the even mode but has little influence on the first even mode f_{e1}. Finally, the coupling length must be in the range of $\lambda_g/4$ (where λ_g is the guided wavelength of the proposed filter at the center frequency) for ensuring a wide bandwidth and flat passband. The coupling lines are kept 0.15 mm apart at the very least. Figure 6 depicts the frequency responses of the BPF, and it can be seen that the performance is excellent in the passband, but the selectivity on both sides of the passband is not favorable.

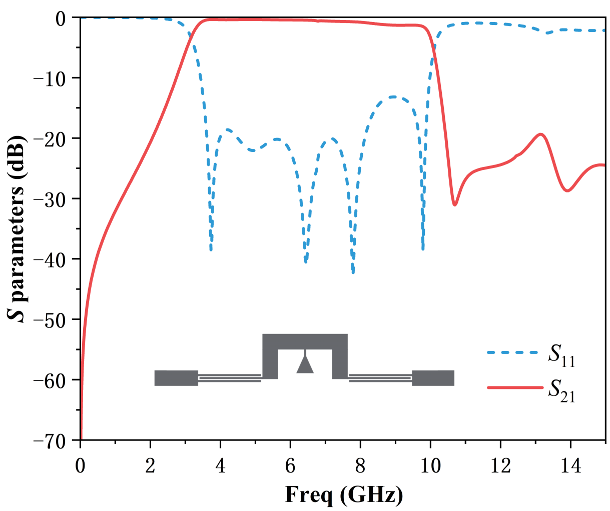

Figure 6. S-parameter simulation without SIRSs.

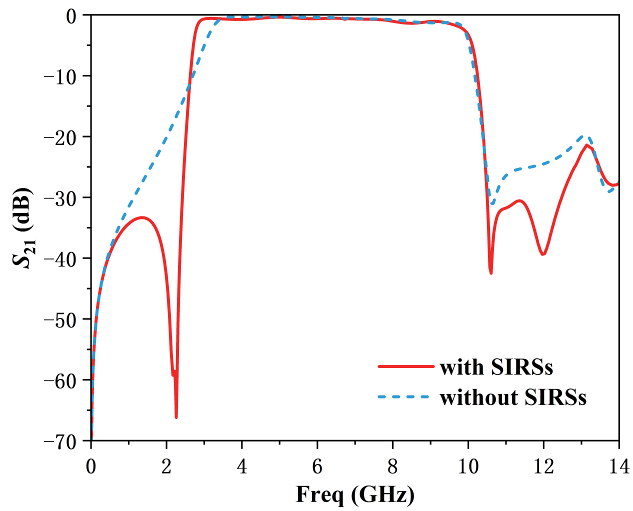

Figure 7. Comparison of transmission characteristics with SIRSs and or not.

Hence, a pair of stepped impedance radial stubs (SIRSs) are developed to generate additional transmission zeros (TZs) in order to significantly enhance the roll-off ratio at the lower and upper passband edges in the UWB [15]. We calculate the lower and upper transmission zeros of the proposed filter as $f_{zl} = 2.2$ GHz and $f_{zh} = 11.9$ GHz, respectively. Finally, Figure 7 illustrates the difference with and without SIRSs. It can be seen that the selectivity on both sides of the filter passband is significantly improved with the addition of SIRSs, where the suppression level of the upper transmission zero, which is at 10.7 GHz and has a 31 dB level, is changed to 42 dB. The current density distributions of the proposed filter at the two transmission zeros frequencies are shown in Figures 8(a) and (b). At the transmission zeros f_{zl} and f_{zh}, the SIRSs have a strong current distribution, and coupling lines are responsible for other transmission zeros in the upper stopband. The physical dimensions of the optimized UWB filter structure are as follows (all in mm): $w_0 = 1.82$, $l_1 = 10.1$, $w_1 = 1.8$, $l_2 = 5.1$, $l_3 = 0.8$, $l_f = 2$, $w_f = 2$, $l_4 = 7.4$, $w_4 = 0.2$, $l_5 = 7.4$, $w_5 = 0.2$, $l_s = 7.26$, $w_s = 0.2$, $r = 4.8$, $\theta = 70°$.

3. EXPERIMENTAL VERIFICATION

Figure 9 illustrates the comparison of the measured frequency response with the simulated data. It can be observed that the 3 dB center frequency of the developed filter is 6.41 GHz, and the 3 dB passband has a fractional bandwidth of 112.5%. The passband insertion loss < 0.55 dB and sharp suppressed skirt edge are caused by the two transmission zeros at the passband edges. The stopband extends till 17 GHz with attenuation better than 20 dB. The group delay (GD) is depicted in Figure 10, from 0.1 to 0.23 ns, which exhibits excellent linearity, and a photograph of the manufactured filter prototype is shown in the inset of Figure 10. Manufacturing flaws, reflections from SMA connectors, and limited substrates are all possible causes of differences between measured data and simulation results. A comparison of the implemented filter architectures with other UWB filters that have been published is shown in Table 1. The results demonstrate that the proposed structure is superior to other structures in terms of edge selectivity, electrical dimensions, and frequency characteristics.

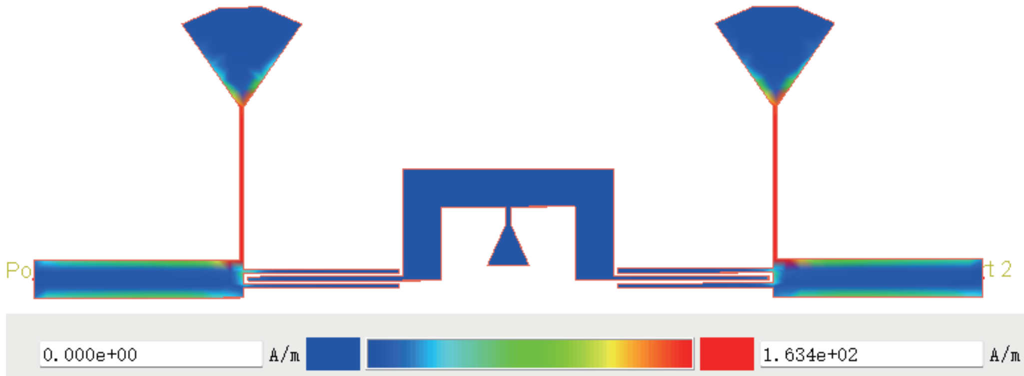

(a)

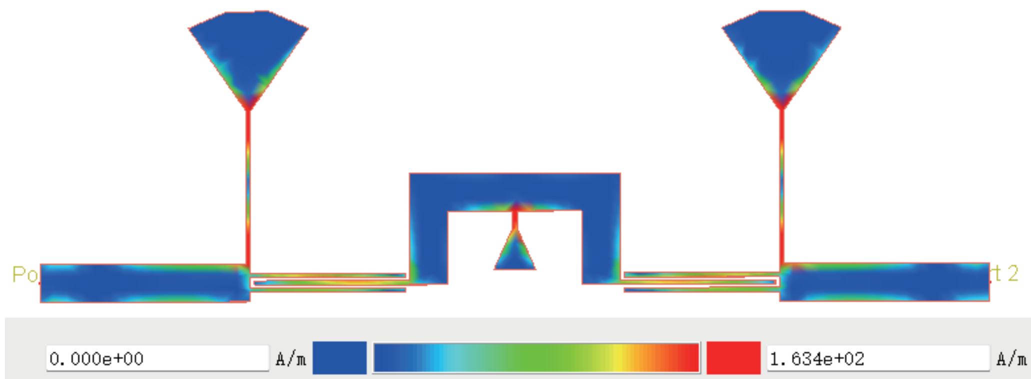

(b)

Figure 8. The current density distribution at (a) 2.2 GHz and (b) 11.9 GHz.

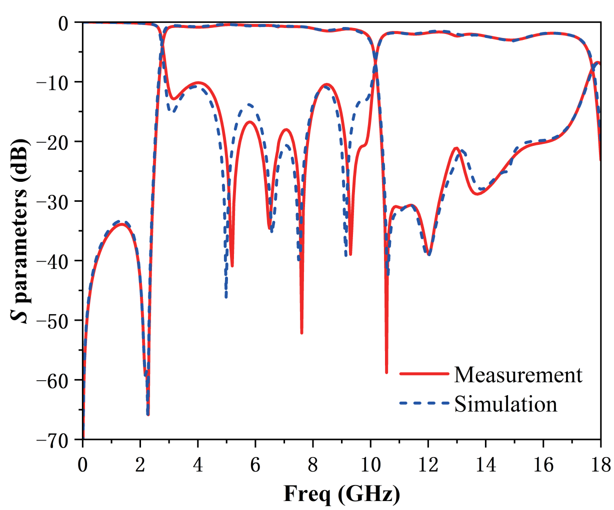

Figure 9. Simulated and measured responses of the proposed filter.

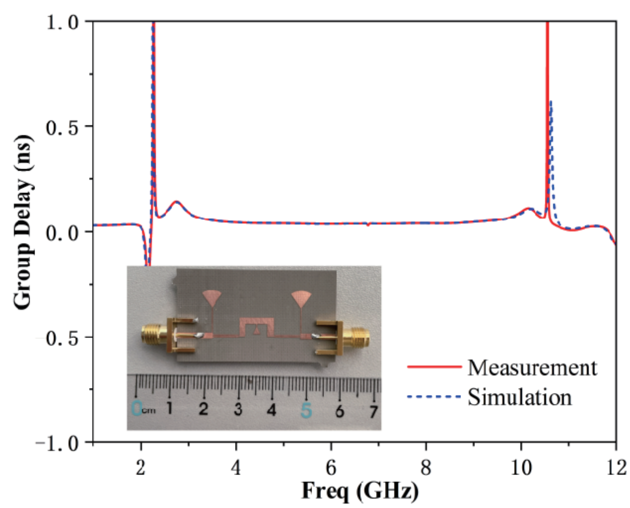

Figure 10. Group delay comparison (manufactured filter in inset).

Table 1. A comparison between the proposed filter and other reported UWB filters.

Ref.	ε_r/height (mm)	GD (ns)	FBW (3 dB)	Roll-off ratio* (dB/GHz), lower and upper	Stopband (GHz)/ attenuation (dB)	size ($\lambda_g \times \lambda_g$)
[5]	3.38/0.508	< 0.17	118	18/19	25/15	0.55×0.3
[6]	2.2/0.787	< 0.5	114	42/48	24/12	1.9×0.44
[10]	3.5/0.508	< 0.8	102	34/41	26.5/23	0.83×0.19
[12]	4.4/0.8	0.11–0.53	118.2	40/46	18/15	0.44×0.33
[13]	10.8/0.635	0.31–0.47	109.6	32/35	17/17	0.5×0.35
This work	3.38/0.8	< 0.13	112.5	99/63	17/20	0.5×0.28

*The roll-off ratio is defined as $27/(|f_{3dB} - f_{30dB}|)$, where f_{3dB} is the 3-dB roll-off frequency and f_{30dB} is the 30-dB stopband edge frequency.

4. CONCLUSION

A novel UWB filter with highly selective performance is presented with a quad-mode resonator (QMR) and open-ended SIRSs. By altering the stub length of the center resonator, the resonant frequencies are uniformly distributed throughout the UWB passband, and a three-line parallel coupling structure is employed to create frequency characteristics with excellent insertion loss and return loss. Two SIRSs were also introduced to produce sharp passband edges. The measured and simulated results are in good agreement. The superior features, such as good frequency characteristics and sharp rejection skirts, demonstrate that the suggested UWB filter is a viable option for UWB systems.

REFERENCES

1. FCC, "Revision of part 15 of the commission's rules regarding ultra-wideband transmission system," *ET-Docket*, 98153, Washington, 2002.
2. Zhu, L., S. Sun, and W. Menzel, "Ultra-wideband (UWB) bandpass filters using multiple-mode resonator," *IEEE Microw. Wireless Compon. Lett.*, Vol. 15, No. 11, 796798, 2005.
3. Li, R. and L. Zhu, "Compact UWB bandpass filter using stub-loaded multiple-mode resonator," *IEEE Microw. Wireless Compon. Lett.*, Vol. 17, No. 1, 4042, 2007.
4. Wong, S. W. and L. Zhu, "Quadruple-mode UWB bandpass filter with improved out-of-band rejection," *IEEE Microw. Wireless Compon. Lett.*, Vol. 19, No. 3, 152154, 2009.
5. Honarvar, M. A. and R. A. Sadeghzadeh, "Design of coplanar waveguide ultrawideband bandpass filter using stub-loaded resonator with notched band," *Microwave and Optical Technology Letters*, Vol. 54, No. 9, 20562061, 2012.
6. Jhariya, D. K., A. Mohan, and M. Sinha, "Design of two-stage fish spear-shaped UWB bandpass filter with sharp selectivity and good out of band performances," *Int. J. Microw. Wireless Technol.*, Vol. 9, No. 9, 1821–1826, 2017.
7. Zhou, C., P. Guo, K. Zhou, and W. Wu, "Design of a compact UWB filter with high selectivity and superwide stopband," *IEEE Microw. Compon. Lett.*, Vol. 27, No. 7, 636–638, 2017.
8. Wong, S. B. and L. Zhu, "EBG-embedded multiple-mode resonator for UWB bandpass filter with improved upper-stopband performance," *IEEE Microw. Compon. Lett.*, Vol. 17, No. 16, 421–423, 2007.
9. Baik, J., S. Han, C. Jeong, J. Jeong, and Y. Kim, "Compact ultra-wideband bandpass filter with EBG structure," *IEEE Microw. Compon. Lett.*, Vol. 18, No. 10, 671–673, 2008.

10. Deng, X., K. D. Xu, Z. Wang, and B. Yan, "Novel microstrip ultra-wideband bandpass filter using radial-stub-loaded structure," *ACES Journal*, Vol. 32, No. 12, 1148–1151, 2017.
11. Abbosh, A., M. Bialkowski, and S. Ibrahim, "Ultra-wideband bandpass filters using broadside-coupled microstrip-coplanar waveguide," *IET Microwaves, Antennas & Propagation*, Vol. 5, No. 7, 764–770, 2011.
12. Ghazali, A. N., M. Sazid, and S. Pal, "A miniaturized low-cost microstrip-to-coplanar waveguide transition-based ultra-wideband bandpass filter with multiple transmission zeros," *Microwave Opt. Technol. Lett.*, Vol. 62, No. 12, 3662–3667, 2020.
13. Ghazali, A. N., M. Sazid, and B. Virdee "A compact UWB-BPF based onmicrostrip-to-CPW transitionwith multiple transmission zeros," *Microwave Opt. Technol. Lett.*, Vol. 6, No. 8, 1925–1928, 2018.
14. Yao, B. Y., Y. G. Zhou, and Q. S. Cao, "Compact UWB bandpass filter using ring open stub loaded multiple-mode resonator," *Electronics Letters*, Vol. 45, No. 11, 554–556, 2009.
15. Jung, M. and B-W. Min, "A highly selective UWB bandpass filter using stepped impedance stubs," *International Journal of Microwave and Wireless Technologies*, Vol. 10, No. 3, 301–307, 2018.